ORIGINAL RESEARCH

Experimental tests on existing RC beams strengthened in flexure and retrofitted for shear by C-FRP in presence of negative moments

Davide Lavorato[1] · Alessandro Vittorio Bergami[1] · Gabriele Fiorentino[1] · Alessandra Fiore[2,3] · Silvia Santini[1] · Camillo Nuti[1,4]

Abstract

The shear strength of reinforced concrete beams extracted from existing buildings often reveals insufficient transversal steel reinforcement, mainly due to design or construction defects or increased design load requirements. FRP wrapping is one of the best solutions to improve beam shear strength as the retrofitting intervention is fast and the cost is modest. Design codes provide clear indication about the retrofitting design of simply supported beams, while the case of a beam with negative moments at the end is not considered, although this is in the case of a beam in a framed structure. One of the main uncertainties lies in the effectiveness of the FRP U sheet anchorage behavior in the area of negative bending moments with cracked concrete. This may limit the shear strength of the retrofitted beam. In this study, two beams extracted from an existing building constructed in the 1930s in Rome and retrofitted by carbon fiber-reinforced polymer (C-FRP) U strips placed at beam ends, where also negative bending moments were present, and have been evaluated with experimental tests at the laboratory of the Department of Architecture of Roma Tre University. Beam steel and concrete characteristics were evaluated by means of different tests. The experimental results are discussed considering the final results in terms of maximum shear resistance in the presence of negative bending moments. Load deflections at different points along the beam, shear-C-FRP deformation along the reinforcement strips and the damage state for different load levels, are presented. The importance of avoiding possible fragile mechanisms in the sections retrofitted with FRP is clearly shown.

Keywords Existing building · RC beams · FRP · Experimental test · Strengthening · End anchorage

Introduction

Recent earthquakes which hit Italy Between August and October 2016 (Fiorentino et al. 2017) demonstrated the high vulnerability of the Italian building stock. This vulnerability is evident for masonry and for reinforced concrete (RC) structures which were designed and built using old design criteria that heavily underestimated the seismic actions.

The use of FRP materials can be a valid solution for the retrofitting of existing RC buildings and bridges (Albanesi et al. 2008, 2009; Lavorato and Nuti 2010, 2011, 2015; Lavorato et al. 2010, 2015, 2017a; Marano et al. 2017).

✉ Camillo Nuti
camillo.nuti@uniroma3.it

Davide Lavorato
davide.lavorato@uniroma3.it

Alessandro Vittorio Bergami
alessandro.bergami@uniroma3.it

Gabriele Fiorentino
gabriele.fiorentino@uniroma3.it

Alessandra Fiore
alessandra.fiore@poliba.it

Silvia Santini
silvia.santini@uniroma3.it

1   Department of Architecture, Roma Tre University, Largo G. B. Marzi 10, 00153 Rome, Italy

2   InGeo, University of Chieti-Pescara "G. d'Annunzio", Viale Pindaro 42, 65127 Pescara, Italy

3   DICAR, Technical University of Bari, Via Orabona 4, 70125 Bari, Italy

4   College of Civil Engineering, University of Fuzhou, No. 2 Xue Yuan Road, University Town, Fuzhou 350108, Fujian, China

🖄 Springer

Many existing RC beams have insufficient shear reinforcement, due to design or construction defects or increased design load requirements. It is worth noting that infill panels can interact with the structural elements and influence their shear strength (Fiore et al. 2016).

The beam retrofitting with carbon fiber-reinforced polymer (C-FRP) sheets or strips is a valid solution to increase the shear strength. The retrofitting intervention with C-FRP is fast and the cost is modest. International and National Guidelines and Codes (CNR-DT 200 R1/2013 2013; Fib 2001; Italian Council of Public Works 2009) give design prescriptions for shear retrofitting of beams by C-FRP which are essentially based on exhaustive experimental data for simply supported beams only.

Key example tests from the literature have been conducted by Pellegrino and Modena (2000), Adhikary and Mutsuyoshi (2004), Carolin and Taljsten (2005), Zhang and Hsu (2005), Barros and Dias (2006), Guadagnini et al. (2006), Monti and Liotta (2007), Bousselham and Chaallal (2008) and Garcez et al. (2008).

In those cases, the new C-FRP shear reinforcements are placed, where moments are negligible and anchored in the compressed upper part of the section in absence of concrete cracking.

RC frames have beams in which the shear forces are combined with negative bending moments at supports with consequent concrete cracking on the upper part of the section (in tension), where the C-FRP anchorages are placed. As a consequence, specific tests are required to validate C-FRP anchorage behavior.

Few studies deal with this issue and new research efforts seem useful. In the scientific literature, Khalifa and Nanni (2000) tested nine continuous two-span beams with different C-FRP amounts and wrapping schemes highlighting that the U-wrap C-FRP reinforcement does not seem to reduce cracks, even if an overall increase of the shear strength is observed.

In the present paper, the behavior of existing RC beams reinforced for shear by C-FRP U strips placed in negative moment sections and anchored under the slab was investigated by experimental tests.

An existing RC building in Rome, dated around year 1930, had to be upgraded to withstand seismic actions and vertical loads according to the Italian Design Code (OPCM 2003; NTC 2008). Although for very extended buildings, as the case study presented herein, there could be spatial variability of the strong motion (Trifunac and Todorowska 1997) which should be taken into account by means of appropriate methods (Lavorato et al. 2017b), this was not taken into account in the retrofitting of this particular building. New RC shear walls and slabs had to be inserted and the application of C-FRP wrapping on existing columns and U-shape strips on beams was necessary for confinement and shear strength, after the construction of an additional slab which increased bending resistance and consequently shear demands.

Two beams were extracted (Fig. 1a, b) and retrofitted as those in the building: same additional slab, longitudinal upper reinforcement, and U-shaped C-FRP strips. After retrofitting, the beams were tested in the PRiSMa Laboratory (Proof Research and testing in Structures and Materials) at Roma Tre University.

The beams were integrated with a new cantilever at one support to reproduce, in the lab, the negative moments and shear due to adequate vertical concentrated loads.

The original removed beams

Geometrical properties and steel reinforcement

The retrofitting intervention on the RC structure involved the construction of new RC walls with consequent removal of two existing beams, as depicted in Fig. 1. These beams, labelled as TM1 and TM2, were carried to the PRiSMa Lab

Fig. 1 Retrofitting of the RC building (**a**) and removal of the beams (**b**)

of the Roma Tre University and retrofitted and tested there. The geometrical properties and the steel reinforcement configuration of the T-section beams TM1 and TM2 with smooth longitudinal rebars and stirrups are given in Table 1.

Material properties

In the following sections, TM1 and TM2 indicate the original beams, while S-TM1 and S-TM2 indicate the beams after the retrofitting interventions. Concrete and steel rebar mechanical characteristics are given in Table 2. Concrete compressive strength is obtained by destructive test on cores extracted after the failure tests on S-TM1, and by SON-REB test on the S-TM2 beam, correlated with core resistances on S-TM1. The characteristics of steel rebars (yield strength, maximum strength, and deformation under maximal load) are evaluated by destructive tests on six samples of smooth rebars removed from the beam TM1 after the failure tests, consisting in three stirrups (2ϕ8 and 1ϕ12) and

three segments of ϕ24 rebars of the longitudinal reinforcement. These reinforcement characteristics can be considered valid for beam TM2 too, being the two beams very close in the building, and given that from direct observation of the specimens, the longitudinal reinforcement seems the same. More information about tests for the mechanical characterization of original beams and retrofitting intervention may be found in Imperatore et al. (2012a, b, 2013a, b), Forte et al. (2018) and Lavorato et al. (2016).

Interventions on the original beams

The intervention consisted in the addition of a cantilever and retrofitting as in the real frame structure building, i.e., for bending and shear. The cantilever was added at one end of the beams to apply negative moments by means of a monodirectional force actuator ("Additional RC cantilever"). Therefore, the two beams have a stress condition which is

Table 1 Geometrical properties and steel reinforcement of beams TM1 and TM2 (mm)

	TM1	TM2	Beam: TM1 (left); TM2 (right)
Beam length (L)	4610	4620	
Average height (H)	525	520	
Width web (b)	260		
Width flange (B)	520	575	
Height flange (h)	210		
Span upper bar	2ϕ24		
Span lower bar	2ϕ24		
Support upper bar	4ϕ24		
Support lower bar	2ϕ24		
Stirrups	17 ϕ8–ϕ12	16 ϕ10	
Stirrups spacing	210–340	210–380	
Long. upper	See picture		
TM1/TM2			
Long. reinforcement			
TM1 stirrups			
TM2 stirrups			

Table 2 Material properties for beams TM1 and TM2

Concrete			Reinforcement					
	f_{cm} (MPa)	Dev. St	Specimen label		ϕ (mm)	σ_y (MPa)	σ_r (MPa)	A_{gt} (%)
TM1	16.38	4.78	Transversal steel	FV_8	8	354.13	472.72	19.64
				FV_12	12	347.61	494.25	9.25
TM2	18.16	–	Longitudinal steel	FV_24	24	265.82	404.87	23.20

Materials properties for beams TM1 and TM2: cylindrical mean compressive strength (f_{cm}) and standard deviation (Dev. St) for concrete; diameter (ϕ), yield stress (σ_y), tensile strength (σ_r) and deformation under maximum load (A_{gt}) for rebar

TM1 data are evaluated on the base of five cores having a diameter of 94 mm and height of 100 mm; TM2 data are obtained by the R_{cm} (mean cubic compression strength) value obtained from SONREB results calibrated on the cylinder tests of the beam TM1

similar to the real building, with simultaneous presence of shear and negative moment at the support.

Then, the beams, TM1 and TM2, with the added cantilever, were retrofitted as in the real building, see Fig. 2, with the construction of an additional RC slab to improve the flexural strength ("Flexural strengthening") and the application of C-FRP strips to enhance the shear strength ("Shear strengthening").

The beam TM1 was tested twice. The first time the beam (labelled S-TM1-A) showed a fragile failure due to collapse of the compressed concrete at the support, and in the added upper slab. Subsequently, the same beam (labelled S-TM1-B) was tested again after adding a new cantilever on the undamaged opposite end with a proper reinforcement in bending for the new slab and the new cantilever and a proper distribution of the connectors between the new and the existing beam slab.

The second beam TM2 was retrofitted, taking into account the previous experience on beam TM1 and tested as S-TM2.

Additional RC cantilever

The cantilever lengths L2 are equal to 1.82 m for the beam S-TM1-A and 1.53 m for the beams S-TM1-B and S-TM2. These differences in the test geometry are due to practical needs for the construction of the cantilevers in the lab, as they were built in different dates. Other differences are in the steel arrangement to improve the reinforcement configuration on the base of the experience acquired during the test on the first beam S-TM1-A.

Concrete class C28/35 (characteristic value of cylinder concrete strength $f_{ck} = 28$ MPa) was used to build the cantilever of the beam S-TM1-A, while it was slightly smaller (average value of cubic concrete strength $R_{cm} = 31.22$ MPa) for the cantilevers of the beams S-TM1-B and S-TM2 (Table 3).

For the S-TM1-A beam, the reinforcement, that is built by a typical B450C steel rebar type (characteristic value of steel

yield strength $f_{yk} = 450$ MPa; see Italian Code NTC 2008), was arranged according to the following scheme:

- longitudinal upper rebars: 4ϕ24 side-welded to the original 4ϕ24 upper rebars of TM1 beam;
- longitudinal lower rebars: 2ϕ12 anchored chemically for a length of 250 mm, drilled in the original beam;
- stirrups: ϕ12/150 mm in the web,
- longitudinal bars 4ϕ12 and stirrups ϕ8/150 mm in the flange.

The reinforcement of the added cantilevers of S-TM1-B and S-TM2 changed in the inferior longitudinal bars and their connection to the existing beam:

- longitudinal upper rebars: 4ϕ18 butt-welded to the upper reinforcement of the existing beams: 4ϕ24;
- longitudinal lower rebars: 2ϕ18 butt-welded to the original lower reinforcement of the existing beam: 2ϕ24;
- stirrups ϕ10/200 mm in the web;
- longitudinal bars 4ϕ12 and stirrups ϕ10/200 mm in the cantilever flange.

The need of a different arrangement in the bottom cantilever reinforcement with respect to S-TM1-A arose after the test of S-TM1-A. In fact, there was failure of bottom concrete of the original TM1 beam which crashed, where cantilever bottom bars, compressed, ended at 250 mm from the support. It was, therefore, decided the butt-welding of the cantilever bottom reinforcement to the bottom reinforcement of the original beam, while larger diameter bars were used, ϕ18 instead of ϕ12, to reduce compression side failure probability. The steel reinforcement of the added cantilever was of the typical B450C type (characteristic value of steel yield strength $f_{yk} = 450$ MPa).

The longitudinal ϕ18 bars and the ϕ24 rebars of the original beams are more or less equivalent in terms of strength, because the yielding strength of B450C steel type is higher with respect to the one of the original smooth rebars. On the
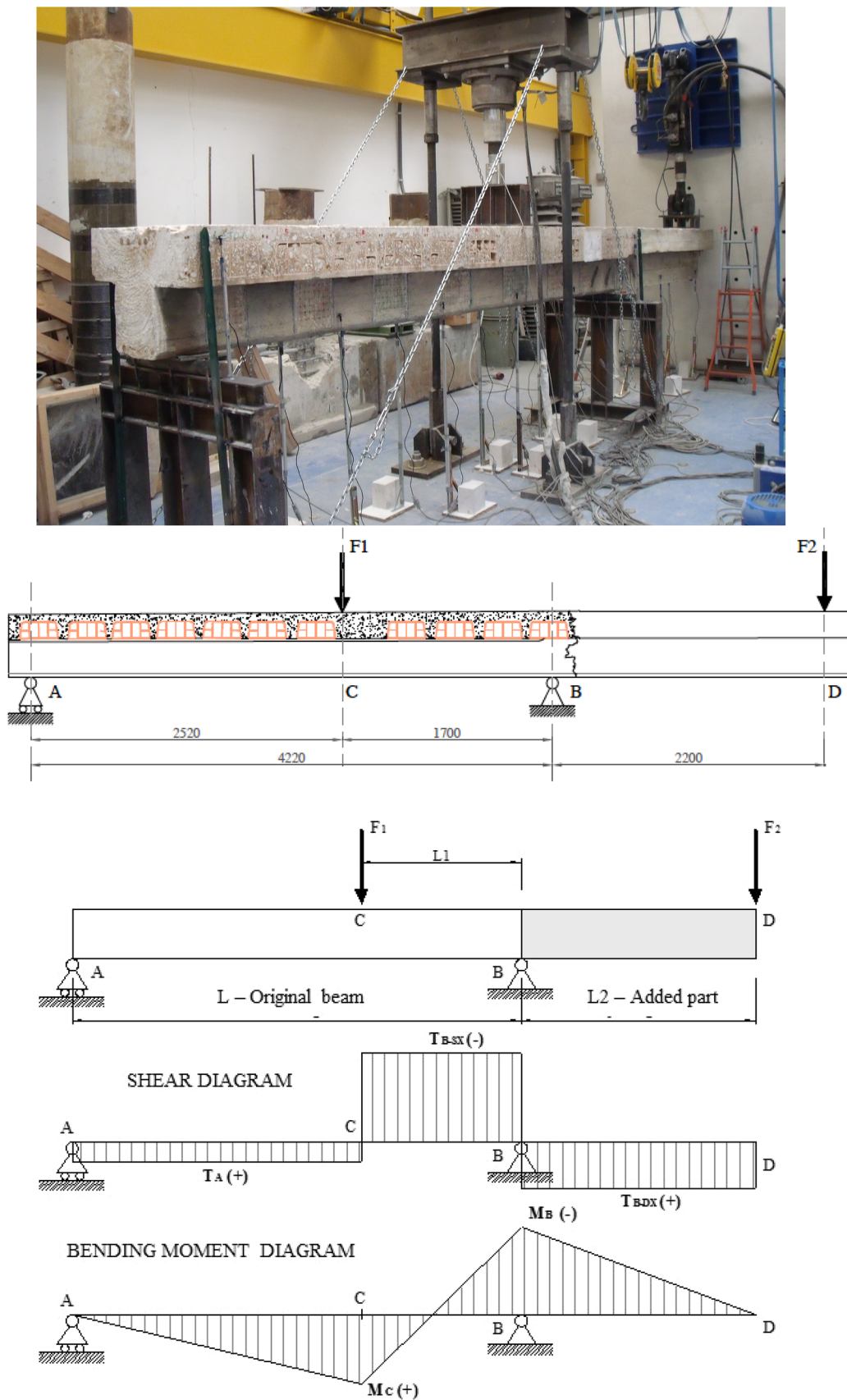
Fig. 2 Beam specimen with added cantilever (top), test load scheme (center) and internal forces (bottom); (mm)

Table 3 Added RC cantilevers: concrete and reinforcement mechanical properties, section geometries

Beam label	Concrete	Reinforcement		Section details
S-TM1-A	C28/35	Trans.	B450C	2Ø12 4Ø24 Ø8/150 2Ø12
		Long.	B450C	Ø12/150 2Ø12
S-TM1-B S-TM2	31.22 Mpa (tested)	Trans.	B450C	2Ø12 4Ø18 Ø10/200 2Ø12
		Long.	B450C	Ø10/200 2Ø18

Trans. transversal steel, *Long.* longitudinal steel reinforcements

other hand, the smaller diameter simplified the butt-welding connection.

Flexural strengthening

The flexural strengthening involves the addition of an RC slab with rectangular section 800 mm wide and 70 mm thick. This slab has been executed in two different ways (Figs. 3, 4). In fact, as already mentioned in the introduction, the original beam TM1 has been subjected to two interventions. The first time the cantilever has been added on one side, then the beam has been strengthened with an additional slab and carbon strips for shear (S-TM1-A), and finally tested to failure. After the removal of the damaged cantilever and slab, a new RC cantilever on the opposite undamaged end of the beam, a new RC slab, and new C-FRP strips have been added for shear resistance (S-TM1-B). A new test has been carried out to failure.

In beam S-TM1-A, the connection between the beam and the additional slab is simply straight vertical rebars $\phi12/200$ mm, see Fig. 3, top and Fig. 4, left, limited to part of the zones of the additional longitudinal reinforcement. These latter consisted in $2+2\,\phi20$, which was limited to the cantilever zone and to the final part of the slab opposite to the cantilever.

The additional slab reinforcement consisted of electro-welded mesh ($\phi8/200\times200$ mm) disposed along the entire RC slab between the lower ($2\,\phi20$) and the upper ($2\,\phi20$) longitudinal rebar layers.

S-TM1-B is obtained from the same beam TM1 after testing S-TM1-A, removing the slab, the cantilever, adding a cantilever on the opposite side and a new slab, with
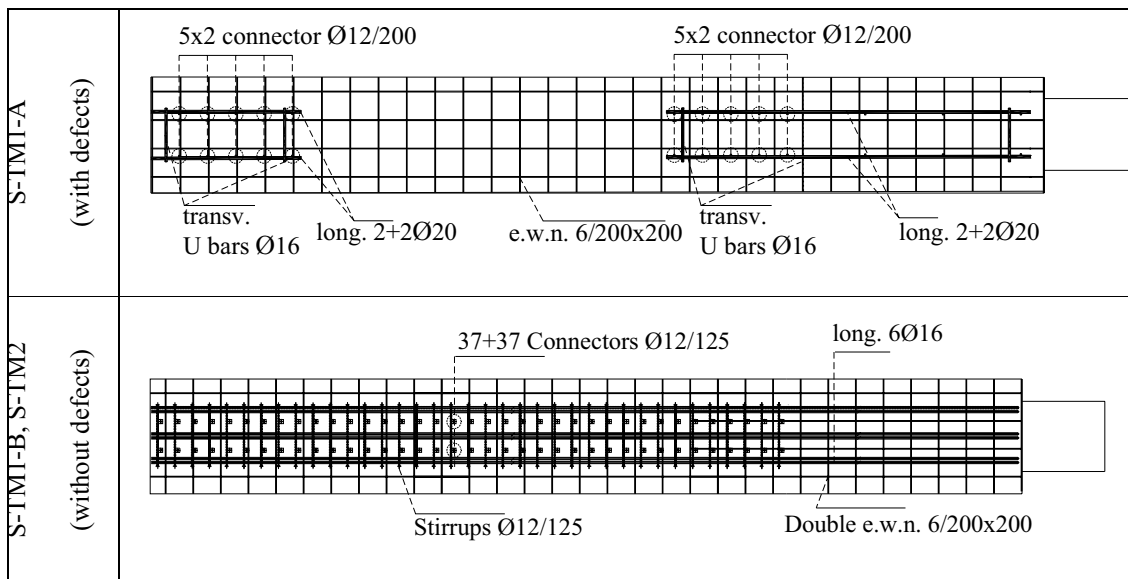
Fig. 3 Retrofitted beams: RC slab steel reinforcement. Beam S-TM1-A (top); beams S-TM1-B and S-TM2 (bottom) (mm)
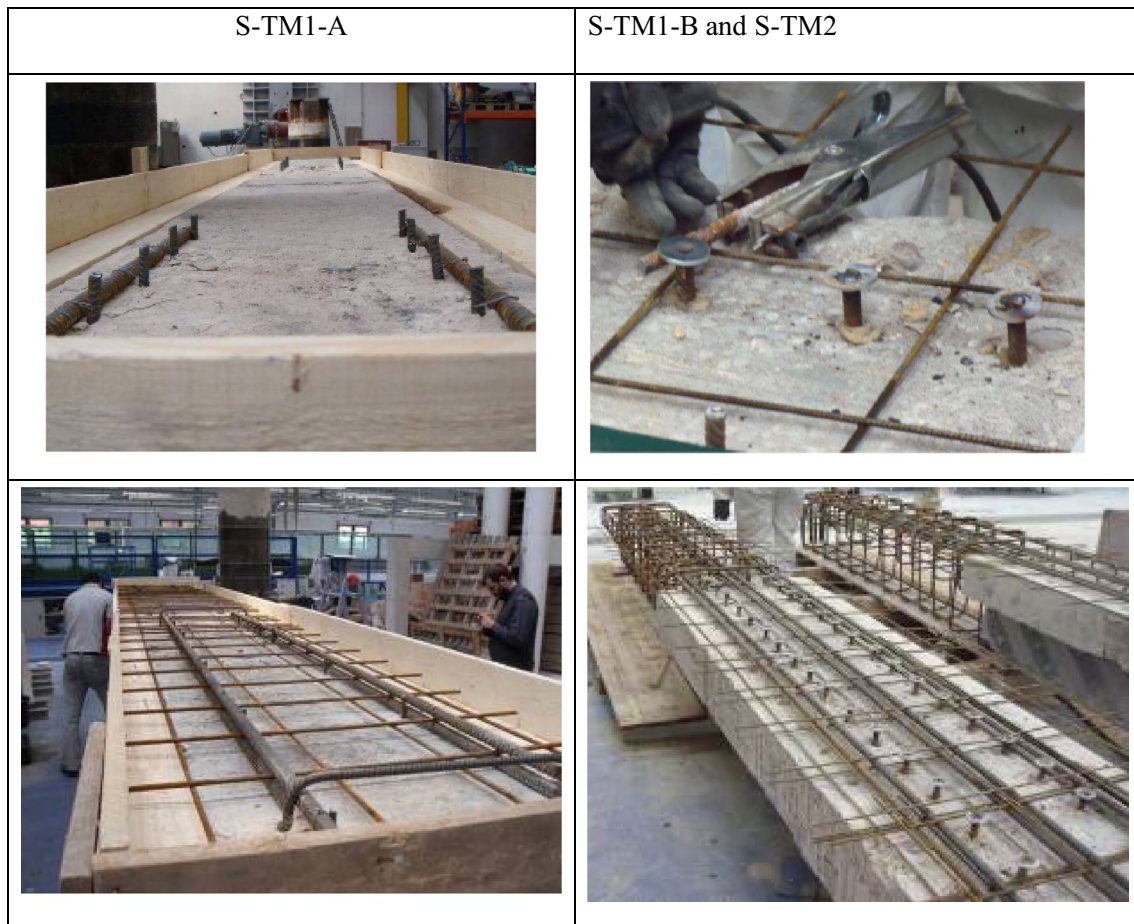
Fig. 4 Retrofitted beams: RC slab steel longitudinal reinforcement, connectors for retrofitted beams S-TM1-A (left), S-TM1-B and S-TM2 (right)

better reinforcement details. For the beam S-TM1-B, the new RC slab had two sets of connectors (ϕ12/125 mm) with butt-welded steel plate and U-shape rebars (as stirrups, ϕ12/125 mm) anchored chemically to connect the new RC slab to the existing one. The connectors, the slab main longitudinal reinforcement (6 ϕ16), and two layers of electro-welded net (ϕ6/200$\times$200 mm, below and above the longitudinal reinforcement) are disposed along the whole length of the beam (Figs. 3, bottom, Fig. 4 right).

The concrete used for the S-TM1-A slab is a lightweight concrete with polypropylene fibers (40$\times$12$\times$0.2 mm) Leca® CLS 1800 with $R_{ck}=45$ MPa according to the commercial datasheet. The concrete is C28/35 type with characteristic cylindrical compressive strength equal to 28 MPa and steel B450C with characteristic yield strength equal to 450 Mpa. The RC slab concrete and steel mechanical characteristics have also been obtained experimentally by failure tests on standard cubic specimens (150 mm side) and steel reinforcement sample (4) if specimens were available. The full mechanical properties of concrete and reinforcement of the new RC slab are given in Table 4.

The RC slab for flexural reinforcement of S-TM1-A had been realized according to the following steps (Fig. 4, left):

1. Anchorage of two sets of connectors ϕ12/200 mm at the beam extrados in correspondence of each beam supports (points A and B, Fig. 2); these connectors were realized with simple rebar segments.
2. Placing of 2 ϕ20 longitudinal rebars in correspondence of each beam supports (points A and B, Fig. 2).
3. Placing of one layer of electro-welded net ϕ8/200$\times$200 mm above the longitudinal rebars.
4. Placing of another 2ϕ20 longitudinal rebars in correspondence of each supports (points A and B, Fig. 2) on the electro-welded net.
5. Casting of lightweight concrete Leca CLS 1800® (http://www.leca.it).

The RC slabs for flexural reinforcement of S-TM1-B and S-TM2 were realized according to the following steps (Fig. 5):

Table 4 Retrofitted beams S-TM1-A, S-TM1-B, and S-TM2: mechanical properties of concrete and reinforcement of the new RC slab

	Concrete	Steel reinforcement			
	R_{cm} (MPa)	Italian class or experimental properties			
RC slab of retrofitted beams					
S-TM1-A	61.70	Connectors	B450C		
			ϕ (mm)	σ_r (MPa)	A_{gt} (%)
		Electro-welded net	8	587.49	8.56
		Long. rebars	20	594.55	12.97
S-TM1-B	31.22	Connectors	B450C		
S-TM2		Electro-welded net	B450C		
		Long. rebars	B450C		

R_{cm} experimental mean compressive strength, ϕ bar diameter, σ_r tensile strength, and A_{gt} deformation under maximum load

- Anchorage of two lines of connectors ϕ12/125 mm along the entire beam extrados; each connector free end has circular butt-welded plate ϕ30 with thickness equal to 5 mm.
- Placing of one layer of electro-welded net ϕ6/200×200 mm along the entire slab.
- Placing of 6ϕ16 longitudinal bars along the entire slab.
- Placing of another layer of electro-welded net ϕ6/200×200 mm along the entire slab.
- Chemical anchorage of stirrups (U-shaped rebars) ϕ12/125 mm along the entire beam extrados.
- Casting of lightweight concrete class C28/35.

Shear strengthening

According to Italian Code (NTC 2008), the shear strength of the reinforced beam [V_{Rd}, Eq. (1)] is equal to the minimum value between strength of the compressed concrete strut ($V_{Rd,c}$) and the sum of the shear strength of the transversal steel reinforcement ($V_{Rd,s}$) and of the C-FRP reinforcement ($V_{Rd,f}$):

$$V_{Rd} = \min\{V_{Rd,s} + V_{Rd,f}, V_{Rd,c}\}. \tag{1}$$

The compressed concrete strut contribution ($V_{Rd,c}$) and the transversal steel contribution ($V_{Rd,s}$) considering a concrete shear crack angle equal to 45°. They result 522 and 80–150 kN (depending on possible stirrups' diameter; see "The original removed beams"), respectively.

The C-FRP reinforcement shear contribution ($V_{Rd,f}$) is calculated by Eq. (2). The required parameters are (see Fig. 6) the thickness (t_f), the width (w_f), the spacing (p_f) of the C-FRP reinforcement, the fiber angle with respect to the beam longitudinal axis (β), the beam effective depth (d), the concrete shear crack angle with respect to the longitudinal beam axis (θ), the effective FRP design strength (f_{fed}), and the partial factor for the resistance model (γ_{Rd}), here assumed as 1:

$$V_{Rd,f} = 1/\gamma_{Rd} \cdot 0.9 \cdot d \cdot f_{fed} \cdot 2 \cdot t_f \cdot (\cot\theta + \cot\beta) \cdot w_f/p_f. \tag{2}$$
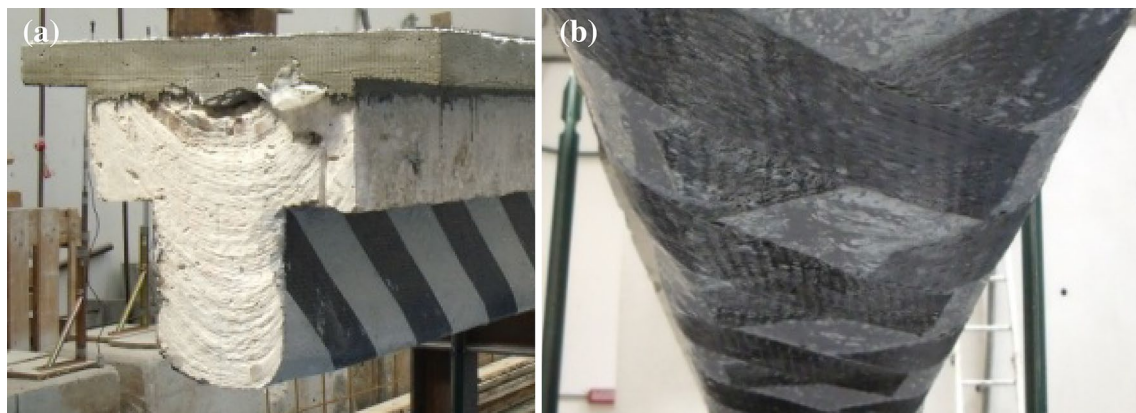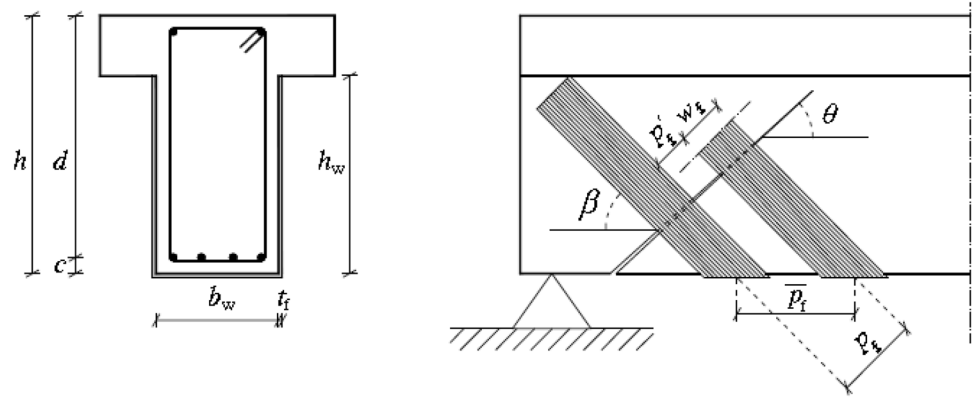

Fig. 5 Retrofitting of the beam specimens: **a** C-FRP strips for shear reinforcement and RC slab for flexural reinforcement; **b** intersection of the C-FRP strips at the beam intrados

Fig. 6 C-FRP shear reinforcement scheme for shear strength evaluation according Italian S.C.P.W guideline (images by Figures 3–8 in Italian Council of public works 2009)

The applied C-FRP shear reinforcement for each beam specimen is made of eight C-FRP U strips (Fig. 6, left) applied along the beam ends for a length of 140 cm starting from both the beam supports. Each U strip is composed by two sheets which cross at 45° on the intrados of the beam (Fig. 6, right). The C-FRP U strips are made of commercial product Carbostru® (https://www.interbau-srl.it) UDHM 400 (weight of 400 g/m^2, tensile strength of 3000 MPa, elastic modulus of 390 GPa, and equivalent thickness $t_f = 0.225$ mm according to the data from technical datasheet). The C-FRP strips have a width $w_f = 100$ mm, the spacing of the strips is $p_f = 212$ mm, and the strips distance is $p_f' = 300$ mm (Fig. 6).

The shear strengthening intervention is made according the "application type A of material and system certification" (CNR-DT 200 R1/2013 2013) and consists in:

1. Mechanical removal of the external grout for a length of 140 cm from the supports.
2. Leveling of the concrete surface.
3. Regularization of the surface by plaster.
4. Application of a thixotropic plaster (epoxy resin, Sikadur-30®, https://ita.sika.com/), having high strength and low shrinkage on the concrete surface.
5. Application of the C-FRP strips using the epoxy resin Carbostru® RS85 (https://www.interbau-srl.it).

The C-FRP strip properties have also been evaluated by qualification tests according to Italian the Code prescriptions called "coupon tests". These consist in tests on C-FRP strips subjected to traction force parallel to the direction of the strips, to simulate the U strips shear behavior. The geometry and mechanical characteristics of the three tested specimens are given in Table 5.

The effective design strength of FRP (f_{fed}) is assumed equal to 541 Mpa, the concrete tensile strength (f_{ctm}) is equal to 2 MPa (a conservative value), and the concrete compressive strength is equal to 16.6 MPa. The concrete strut angle is equal to 45° according to Italian Code prescription and the safety coefficients $\gamma_{f,d}$, γ_c, and $\gamma_{R,d}$ are assumed equal to 1. The resulting C-FRP reinforcement theoretical shear strength [$V_{Rd,f}$, Eq. (2)] results equal to 116 kN.

The two resulting shear strength values for the beam ($V_{Rd,s} + V_{Rd,f}$) considering the two possible stirrups' arrangements (see "The original removed beams") and so the two possible values of the stirrups' shear contributions ($V_{Rd,s} = 80$–150) results equal to 196–266 kN. The large scatter for the stirrups' shear contributions depends on the possible stirrup diameter. The stirrups' rebar diameter is difficult to evaluate by non-destructive tests.

Tests: set up for loadings and applied load histories

Two set of tests are presented: the first one was carried out after the construction of the cantilever to evaluate the stiffness of the beam in the elastic field before retrofitting and the second one was performed until failure to check the ultimate behavior of the retrofitted beams. The latter was performed with special attention on the behavior of the C-FRP strip

Table 5 C-FRP coupon geometry and mechanical properties width (b), thickness (s), fiber area (A_{fib}), composite area (A_{com}), failure force (F), maximum deformation (ε_{max}), fiber stress (σ_{r-fib}), composite stress (σ_{r-com}), fiber elastic modulus (E_{fib}), and composite elastic modulus (E_{com})

Specimen	b (mm)	s (mm)	A_{fib} (mm^2)	A_{com} (mm^2)	F (kN)	ε_{max} (%)	σ_{r-fib} (MPa)	σ_{r-com} (MPa)	E_{fib} (GPa)	E_{com} (GPa)
T_01	16.30	4.1	10.76	66.2	28.24	0.7846	2625.02	426.73	335	54
T_02	17.70	3.7	11.68	66.0	28.11	0.6660	2406.61	425.83	361	64
T_03	18.45	3.7	12.18	68.8	44.78	0.8435	3677.66	650.74	436	77

contribution to beam shear strength at support B, where the C-FRP reinforcement was anchored in a zone with negative bending moment. Some details about the tests are reported in Nuti et al. (2010, 2014).

The simply supported beam with cantilever is an isostatic load scheme, and therefore, internal forces, bending moment, and shear depend on the position and intensity of the external applied loads only, as shown in Fig. 2. Two loads have been applied: $F1$ on the beam span and $F2$ on the cantilever end. They are increased in steps to obtain at each loading step the desired values of shear and moment at support B.

The span load $F1$ is placed at a distance $L1$ from support B (see Fig. 7) between $2.5 H$ and $3 H$ (H is the beam section height, Table 1), which determine shear failure without arch mechanism. $F2$ is applied at the cantilever end, i.e., at $L2$ (see Fig. 7).

Experimental setup for loading and measurements

The test apparatus reproduces the load scheme in Fig. 2. The beam specimens were placed on two steel frames (supports A and B). The load $F1$ is applied on the beam span by a 1000 kN hydraulic jack (300 mm maximum stroke) controlled by an external load cell (1000 kN maximum load, TEDEA-HUNTLEIGH). The load $F2$ is applied on the cantilever end by a 250 kN MTS hydraulic actuator (250 mm maximum stroke) controlled by an internal load cell and the Labview® (http://www.ni.com/it-it/shop/labview.html) software for the application of load or displacement histories. The acquisition system consisted of:

- National Instruments DAQ station SCXI 1001 with DAQ moduli SCXI 1314/1520.
- National Instruments DAQ board 6281 (18 bit).
- LabView acquisition program.

The beam deflections and the C-FRP strains acquisition system consisted of:

- 24 potentiometers Penny–Giles on the two beam sides (10 with stroke ± 25.0 mm and 14 with stroke ± 50.0 mm); 12 potentiometers for the beam vertical displacements along the span at 0.2–0.4–0.6 L (load $F1$ application point)—0.8 L from the simple support without cantilever and along the cantilever at 0.5 $L2$—$L2$ (load $F2$ application point) (Fig. 7); four potentiometers for the beam support vertical displacements; and eight potentiometers for the beam shear deformations (diagonal direction) beside the C-FRP strips
- 18 strain gauges (10 mm grid) placed at 45° on the C-FRP strips $f4$, $f3$, $f2$, and $f1$ (Fig. 7) near support B (six for strip and three for each side).

Load steps for elastic tests before retrofitting

The loading in the elastic test had the aim of not overtaking 80% of shear resistance of the beams, as given in Table 6. The loading steps are given in Fig. 8. The corresponding moment and shear are given in Table 7. Note that in the final step, the internal shear force is 71 kN, about 80% of the theoretical strength. The corresponding bending moment is well below the bending resistance.

Load steps for failure tests on the retrofitted beams

The bending moment strength (M), based on the geometry and reinforcement characteristics, in the span and at support B (M_{uC}, M_{uB}) and the design goal shear resistance (V_u) at the left of support B are given in Table 8.
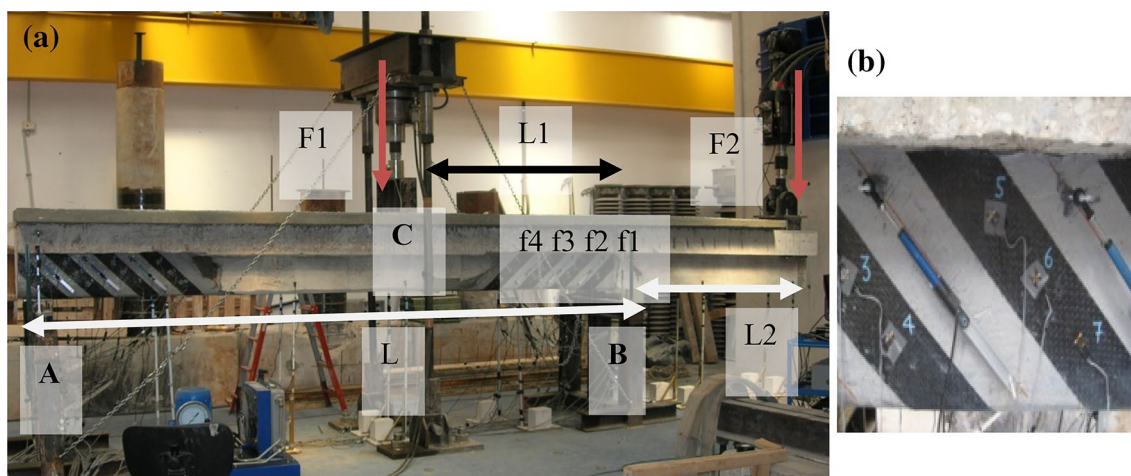

Fig. 7 Retrofitted beams in test apparatus: **a** retrofitted beams in the test apparatus; **b** potentiometers and strain gauges on the C-FRP strips

Table 6 Theoretical bending and shear strength of the beams before retrofitting (assuming 8 mm for stirrups' diameter)

Beam	M_{uc} (kN m)	M_{ub} (kN m)	V_u (kN m)
TM1	254	248	89
TM2	251	243	87

Table 8 Theoretical bending resistance at mid-span and bending and shear resistance at left of support B after retrofitting

Beam	M_{uC} (kN m)	M_{uB} (kN m)	V_u (kN)
TM1	291	457	215

Loading steps differ among the two elastic tests before retrofitting and tests to failure after retrofitting, because the geometry of the loads was different. Small difference in the geometries of beam S-TM1-A and the couple S-TM1-B, S-TM2, existed as well, therefore, the loading steps were slightly different.

The goal of the failure test for each beam is the evaluation of the bending and shear strength on the left side of beam support B.

The geometry of the failure tests on S-TM1-A and on the S-TM1-B and S-TM2 beams are given in Figs. 9 and 10, respectively.

Load steps applied on the S-TM1-A during the failure test are given in Table 9. The load steps are interrupted

below the values $F2 = 140$ kN and $F1 = 254$ kN, required to give the intended shear and bending moment on the left of the support B (shear 215 kN and bending moment 457 kN m), as the beam failed in bending for various inadequate detailing discussed in test results ("Experimental results").

The last load steps were N. 11 with $F1 = 180$ kN and $F2 = 100$ kN and N. 12 with $F1 = 201$ and $F2 = 118$ kN. One can see that in steps N. 12A and 12B, we could increase $F1$, but not $F2$ due to bending failure of the support.

Load steps applied on the S-TM1-B and S-TM2 during the failure test are practically coincident and are given in Table 10.
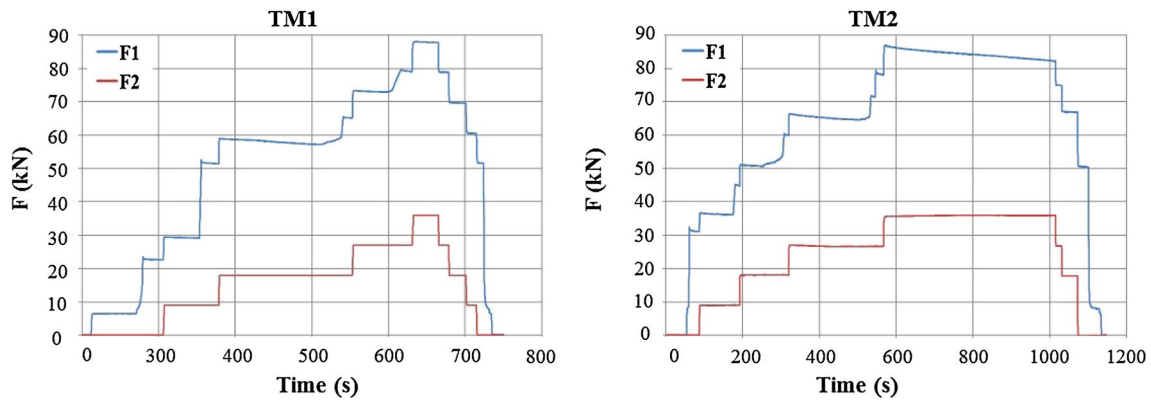
Fig. 8 Elastic test load history: $F1$ (blue solid line) and $F2$ (red solid line) are the forces applied on the beam according to the load scheme displayed in Fig. 7

Table 7 Loading steps for the external forces $F1$ and $F2$ (F_{1hyp}: desired applied; F_{1ef}: effectively applied load) and corresponding internal forces (shear T, bending moment M) at beam support B and C in the elastic tests before retrofitting

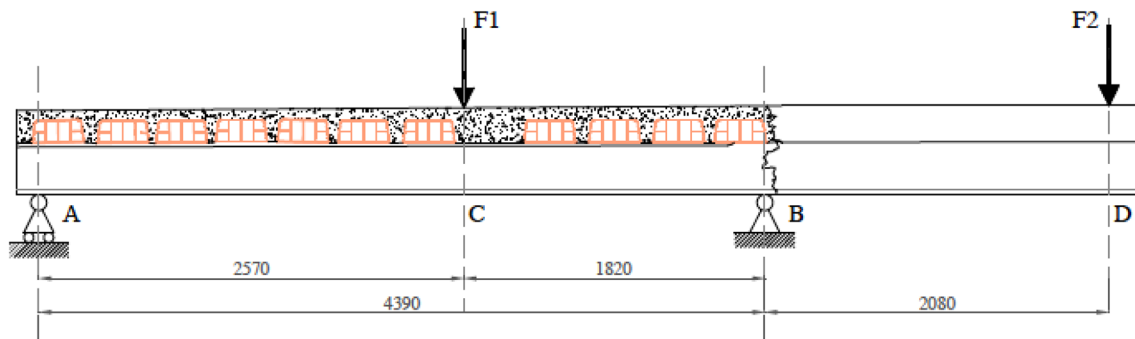| Step	F_{1hyp} (kN)	TM1					TM2				
		F_{1ef} (kN)	F_2 (kN)	T_{Bsx} (kN)	M_C (kN×m)	M_B (kN×m)	F_{1ef} (kN)	F_2 (kN)	T_{Bsx} (kN)	M_C (kN×m)	M_B (kN×m)
1	20.00	23.00	0.00	− 13.73	23.35	0.00	32.00	0.00	− 19.11	32.49	0.00
2	20.00	29.50	9.00	− 22.32	18.10	− 19.85	36.00	9.00	− 26.20	24.70	− 19.85
3	40.00	52.50	9.00	− 36.05	41.45	− 19.85	45.00	9.00	− 31.57	33.83	− 19.85
4	40.00	58.00	18.00	− 44.04	35.18	− 39.69	51.00	18.00	− 39.86	28.07	− 39.69
5	60.00	64.50	18.00	− 47.92	41.78	− 39.69	60.00	18.00	− 45.23	37.21	− 39.69
6	60.00	73.00	27.00	− 57.70	38.56	− 59.54	66.00	27.00	− 53.52	31.45	− 59.54
7	80.00	79.00	27.00	− 61.28	44.65	− 59.54	80.00	27.00	− 61.88	45.66	− 59.54
8	80.00	88.00	36.00	− 71.36	41.93	− 79.38	87.00	36.00	− 70.76	40.92	− 79.38

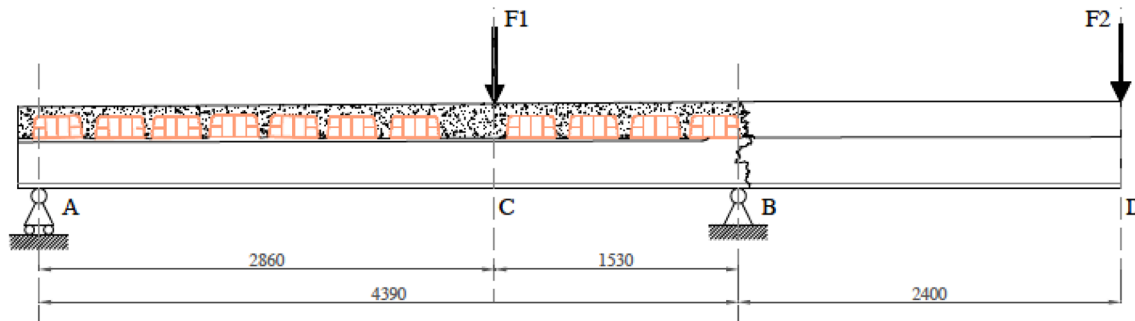**Fig. 9** S-TM1-A failure test scheme after retrofitting

Fig. 10 S-TM1-B and S-TM2 failure test scheme after retrofitting

Table 9 S-TM1-A loading steps and corresponding internal forces in the elastic tests before retrofitting

Step	F_1^{hyp} (kN)	TM1							
		F_1^{ef} (kN)	F_2 (kN)	T_{Bsx} (kN)	T_{Bsx}/T_{Bu} (%)	M_C (kN×m)	M_C/M_{Cu} (%)	M_B (kN×m)	M_B/M_{Bu} (%)
1	20.00	24.40	0.00	− 14.28	6.60	26.00	8.93	0.00	0.00
2	20.00	35.90	20.00	− 30.49	14.18	13.90	4.77	− 41.60	9.10
3	50.00	47.90	20.00	− 37.52	17.45	26.68	9.17	− 41.60	9.10
4	50.00	61.90	40.00	− 55.19	25.67	17.25	5.93	− 83.20	18.21
5	80.00	79.00	40.00	− 65.20	30.32	35.46	12.18	− 83.20	18.21
6	80.00	92.50	60.00	− 82.58	38.41	25.50	8.76	− 124.80	27.31
7	110.00	108.60	60.00	− 92.01	42.80	42.65	14.66	− 124.80	27.31
8	110.00	123.60	80.00	− 110.26	51.28	34.28	11.78	− 166.40	36.41
9	145.00	143.70	80.00	− 122.03	56.76	55.69	19.14	− 166.40	36.41
10	145.00	160.50	100.00	− 141.34	65.74	49.24	16.92	− 208.00	45.51
11	180.00	178.50	100.00	− 151.88	70.64	68.42	23.51	− 208.00	45.51
12	180.00	201.00	118.00	− 173.58	80.73	70.47	24.22	− 245.44	53.71
12A	–	219.40	111.92	− 181.47	84.40	97.48	33.50	− 232.79	50.94
12B	–	239.50	73.30	− 174.94	81.36	165.92	57.02	− 152.46	33.36

F_1^{hyp} desired applied, F_1^{ef} effectively applied load

Table 10 S-TM2 loading steps and corresponding internal forces in the elastic tests before retrofitting

Step	F_1^{hyp} (kN)	TM2							
		F_1^{ef} (kN)	F_2 (kN)	T_{Bsx} (kN)	$T_{\text{Bsx}}/T_{\text{Bu}}$ (%)	M_{C} (kN×m)	$M_{\text{C}}/M_{\text{Cu}}$ (%)	M_{B} (kN×m)	$M_{\text{B}}/M_{\text{Bu}}$ (%)
1	50.00	50.71	0.00	−33.04	16.04	50.55	15.12	0.00	0.00
2	50.00	57.33	15.00	−45.55	22.11	33.69	10.08	−36.00	8.29
3	100.00	102.09	15.00	−74.71	36.27	78.31	23.43	−36.00	8.29
4	100.00	110.37	30.00	−88.30	42.87	63.11	18.88	−72.00	16.59
5	150.00	152.78	30.00	−115.93	56.28	105.38	31.53	−72.00	16.59
6	150.00	171.58	60.00	−144.58	70.19	77.21	23.10	−144.00	33.18
7	200.00	201.80	60.00	−164.27	79.74	107.33	32.12	−144.00	33.18
8	200.00	218.58	85.00	−188.87	91.68	84.97	25.43	−204.00	47.00
9	250.00	251.39	85.00	−210.24	102.06	117.67	35.21	−204.00	47.00
10	250.00	254.64	100.00	−220.56	107.07	97.46	29.16	−240.00	55.30
11	300.00	301.56	100.00	−251.13	121.91	144.23	43.16	−240.00	55.30
12	300.00	302.31	115.00	−259.82	126.13	121.52	36.36	−276.00	63.59
13	350.00	351.24	115.00	−291.70	141.60	170.30	50.96	−276.00	63.59
14	350.00	357.52	130.00	−303.99	147.57	153.10	45.81	−312.00	71.89
15	400.00	401.71	130.00	−332.78	161.54	197.15	58.99	−312.00	71.89
16	400.00	400.09	145.00	−339.92	165.01	172.08	51.49	−348.00	80.18
17	450.00	450.85	145.00	−372.99	181.06	222.68	66.63	−348.00	80.18
18	450.00	456.71	165.00	−387.74	188.22	197.25	59.02	−396.00	91.24
19	500.00	500.84	165.00	−416.49	202.18	241.23	72.18	−396.00	91.24
19A	500.00	444.38	165.00	−379.71	184.33	184.96	55.34	−396.00	91.24
20	500.00	452.30	176.40	−391.10	189.86	175.03	52.37	−423.36	97.55
21	–	454.78	132.00	−368.44	178.86	246.92	73.88	−316.80	73.00

The loading steps for S-TM1-B are practically coincident and so the table is omitted

F_1^{hyp} desired applied, F_1^{ef} effectively applied load

Experimental results

The experimental results about the elastic and failure tests described in §4 are discussed in terms of: (1) behavior (deflections) of the non-retrofitted beams during the elastic tests and (2) behavior (deflections and C-FRP reinforcement deformations) of the retrofitted beams during the failure tests.

The latter test results are discussed to evaluate the real C-FRP contribution to the shear strength of the retrofitted beam in term of: the ratio between the theoretical and the experimental beam shear strength and the additional contribution of the C-FRP shear reinforcement to the total beam shear strength, the so-called C-FRP efficiency.

Preliminary elastic tests on the no retrofitted beams with the added cantilever

The obtained beam deflections under the maximum loads during the elastic tests on S-TM1 and S-TM2 beams are given in Fig. 11. The comparison between the two beams deflections showed that beam S-TM1 had larger mid-span and cantilever displacements.

Displacements under $F1$ at point C in Fig. 11 are from 35% (S-MT1) to 25% (S-MT2) larger than those calculated with the gross section without considering the cracking state before the test.

Failure test on beam S-TM1-A failure happened in a premature manner at a shear $T_{\text{Bsx}} = 174$ kN with a negative moment of 245 kN m. We remember that the goal shear was 215 kN and bending moment of 457 kN m.

The experimental behavior of the specimen S-TM1-A enhanced the ineffectiveness at failure of the new concrete slab due to the absence of efficient connectors and abrupt interruption of longitudinal reinforcement. The additional slab lifted from the beam near support B at a load $F1 = 150$ kN, as the connector added for the slab had no anchoring device at the end and loosed vertical connection with concrete.

Beam deflections

The behavior of the beam compared to that before retrofitting can be seen in Fig. 12 in terms of beam deflections. As already explained, the geometry of failure tests has light differences with respect to the elastic one. Therefore,

Fig. 11 Deflections along the beams S-TM1 and S-TM2 under the loads $F1 = 79$–80 kN and $F2 = 27$ kN during the elastic tests
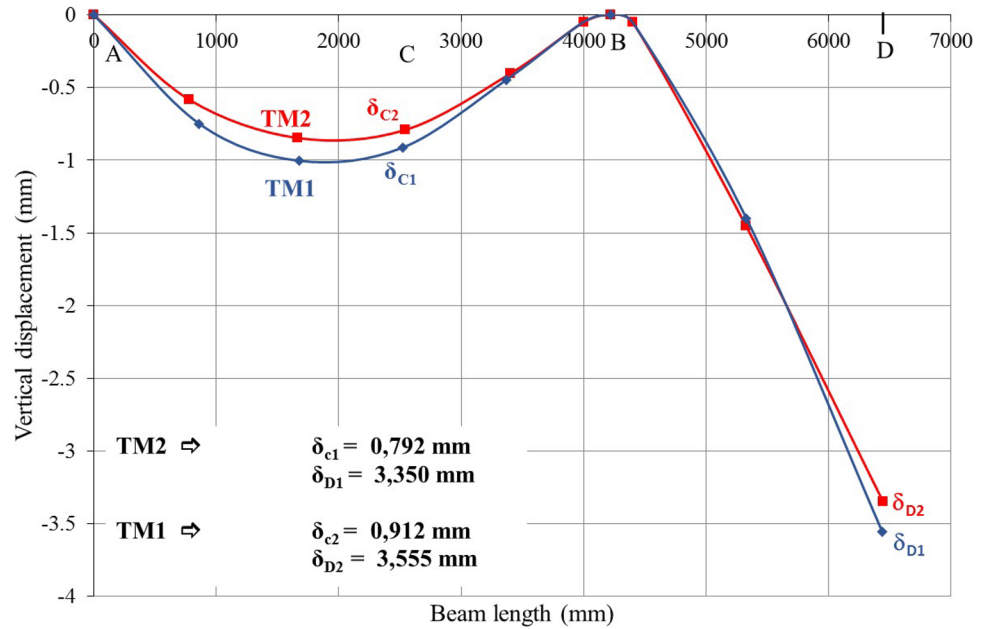
Fig. 12 Deflections of the beam S-TM1-A for loads $F1 = 73$–75 kN and $F2 = 27$ kN before retrofitting (TM1pre) and after retrofitting (TM1post)
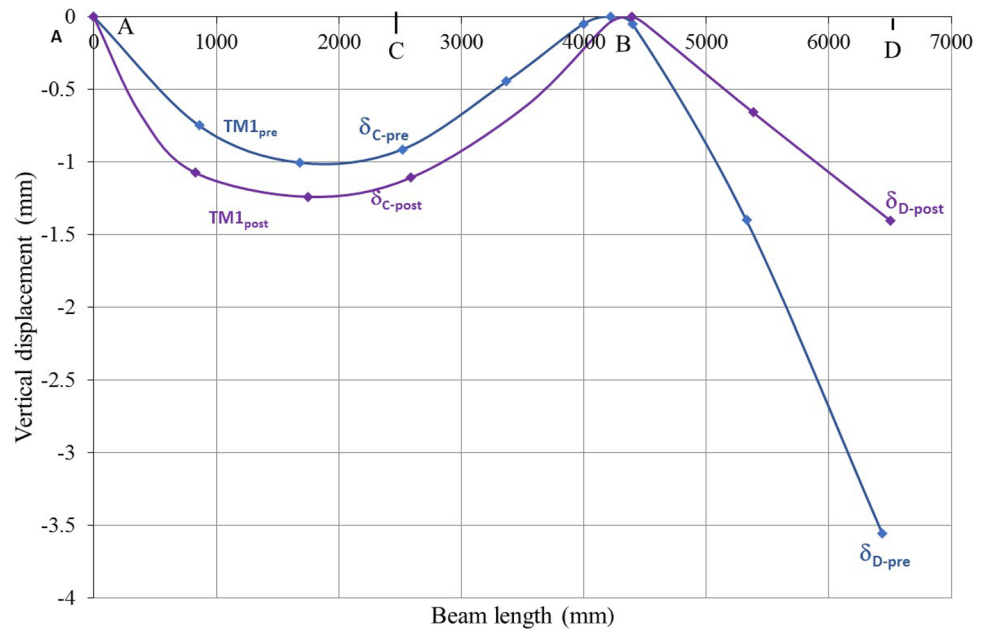

displacement comparison is not straightforward. The span of the retrofitted beam is larger, while the cantilever is shorter. Therefore, larger span and smaller cantilever displacements were expected.

Figure 13 shows the results of the failure test carried on on retrofitted beam S-TM1-A. Passing to larger forces, the deflection direction and the beam stiffness changed abruptly when the load $F1$ was equal to about 180 kN and $F2$ about 100 kN. The corresponding shear force was 152 kN and the bending moment was 200 kN m. At the following step with $F1 = 200$ kN and $F2 = 118$ kN, corresponding to a shear force of 173 kN and a moment of 254 kN m, there was total failure. Failure happened in a brittle manner due to flexure at support B with concrete crushing and detachment of C-FRP reinforcement.

This should have been foreseen as the section is strongly reinforced in tension with few compressed steel badly anchored (See Fig. 3) .
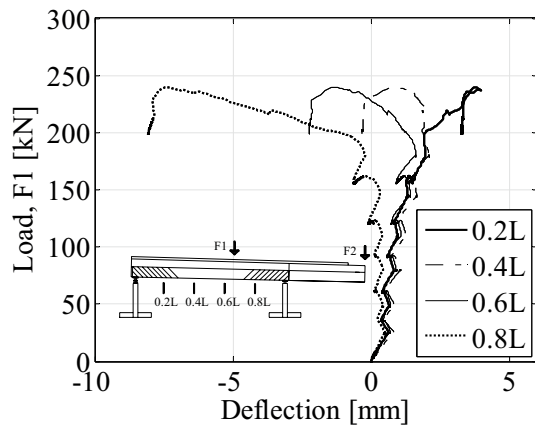
Fig. 13 Retrofitted beam S-TM1-A experimental results of the failure test: load $F1$ vs span deflection curves at 0.2, 0.4, 0.6 and 0.8 L

C-FRP deformations

The shear at support B (T_B) VS deformation of C-FRP of the strips $f2$, $f3$, and $f4$ at their top, middle, and bottom points is shown in Fig. 14. The beam design shear strength (215 kN) was, by far, not obtained. The contribution of C-FRP strips was well below the expected design one (116 kN). However, the deformations of the C-FRP strips were modest due to the detachment of the concrete base due to the ejection of concrete cover at the anchorage of the strips nearest to support due to bending failure of the beam with concrete crushing (Fig. 15). For that reason, the C-FRP shear reinforcement could not develop its contribution.

Failure mechanism

Failure was evident as various fragile mechanism arose. The additional slab detached, lifting upward from the original beam, near support B, as the connectors were not adequately anchored at their top. The longitudinal new slab rebars were interrupted all together in the slab causing, at the interruption section, the rupture of the slab in tension, while the slab lifted from the original beam (see Fig. 15). Flexural reinforcement was not effective near the support B. The new cantilever had bottom reinforcement anchored in the old beam with a short superposition. This detail caused the total inefficiency of bottom reinforcement which rendered the section sensible to brittle failure and caused rupture by crushing of compressed concrete at support B with buckling of the longitudinal rebars and detachment of the C-FRP reinforcement (Zhou et al. 2014, 2015). For that reason, the shear retrofitting was not effective.

The beam damage developed seriously near support B, starting from a shear (T_B) of 141 kN and a moment (M_B) of 208 kN m ($F1 = 160$ kN and $F2 = 100$ kN), and included:

- evident vertical cracks on the original beam flange;
- detachment and lifting of the new RC slab (max lifting = 6 cm);
- concrete crushing along the beam sides at the support B near the connection with the cantilever with primer (on which C-FRP strips are applied) damage.

Finally, wide diagonal shear cracks appeared along the original beam flange. The collapse occurred when the shear T_B was 181.47 kN and the moment M_B was 232.79 kN m ($F1 = 219.4$ kN, $F2 = 111.92$ kN), as displayed in Fig. 15. These actions values were smaller than the design ones, in particular the shear of about 10–20%. The segment of the beam from the support A to the section of the applied load $F1$ presented no significant damage at beam failure. This permitted to reuse of the beam TM1 with a new cantilever starting from A.

Failure test on beam S-TM1-B and S-TM2

Beam deflections

The two beams S-TM1-B and S-TM2 showed greater strengths than the design ones (Fig. 16). They had similar initial stiffness and yielding deformations. They also showed significant deformation capacity, as demonstration of the good retrofitting detailing now adopted, validating the final design solution.

Beam S-TM1-B, already tested as S-TM1-A, showed plateau strength only (450 kN) without initial peak value (500 kN) like in S-TM2. This was probably due to the damage cumulated in S-TM1-A beam failure test. The total displacement was, however, large in both, with values of about 15–20 mm at 0.4 and 0.6 L.

Beam S-TM2 had a peak strength at the displacement of 7.5 mm at 0.4 and 0.6 L, after a couple of mm the force reduced to about 400 kN. This value remained constant to failure with 33–43 mm of displacement.

The beam collapse resulted plastic as a good design has to guarantee.

C-FRP deformations

The C-FRP deformations are given in Figs. 17 and 18 for each strip ($f2$–$f3$–$f4$) on the two beam sides, as a function of internal shear force.

The maximum experimental C-FRP deformations were in range of 1.0‰ (in one point 1.5‰, strip 4) for S-TM1-B (Fig. 17) and in the same range 1.0‰—(but maximum of
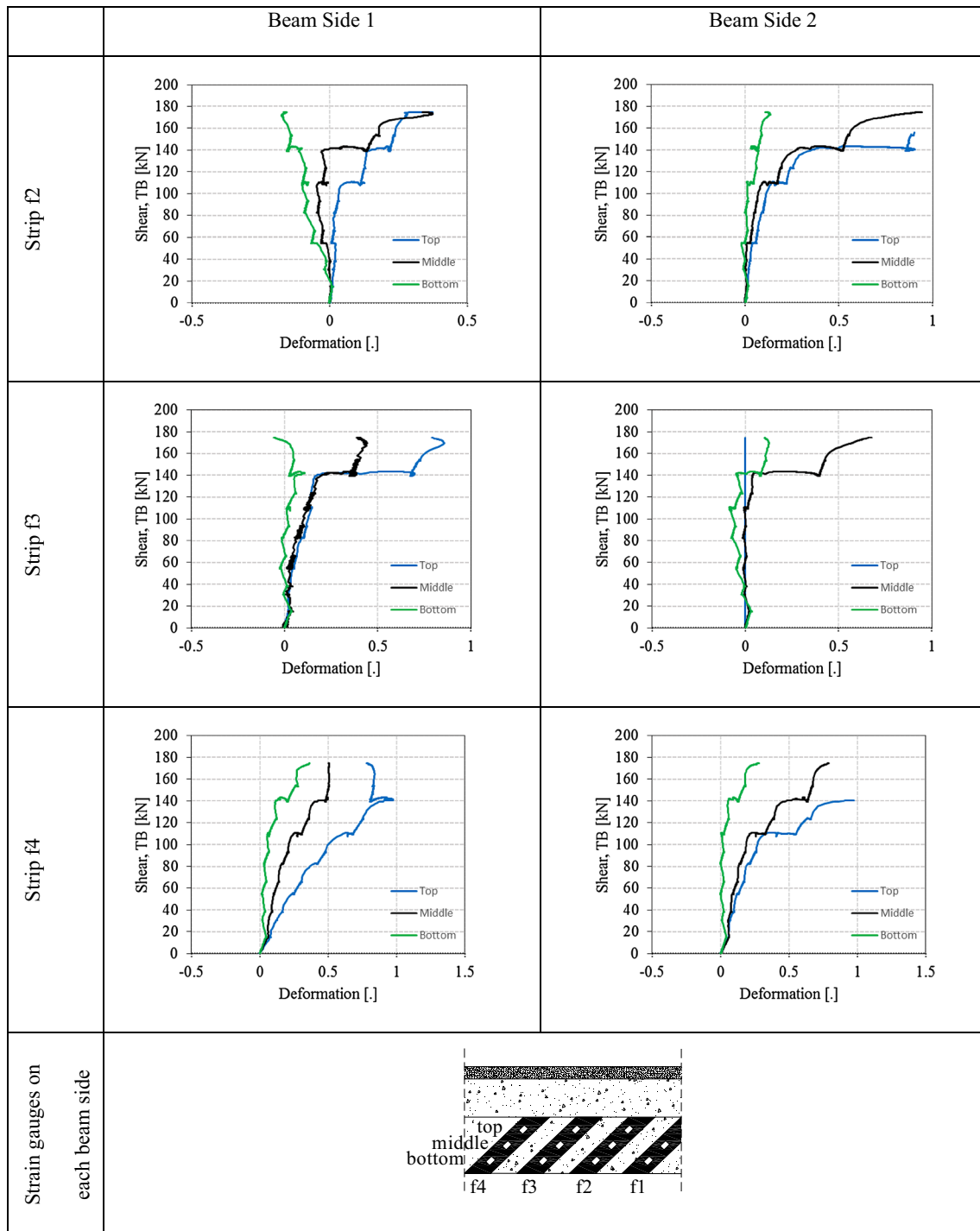
Fig. 14 Retrofitted beam S-TM1-A experimental results of the failure test: shear at support B vs deformation for the C-FRP strips $f2$, $f3$, $f4$ measured by strain gauges at the top, middle and bottom positions on each beam side

2.0‰ but in strip 2) for S-TM2 (Fig. 18). These values were significantly smaller than the one assumed during the C-FRP reinforcement design (5‰).

Failure of the C-FRP reinforcement was due to debonding of the strips starting from a shear value of 375–400 kN for S-TM1-B and S-TM2 beam, respectively. These shear values were greater than the retrofitting objective;
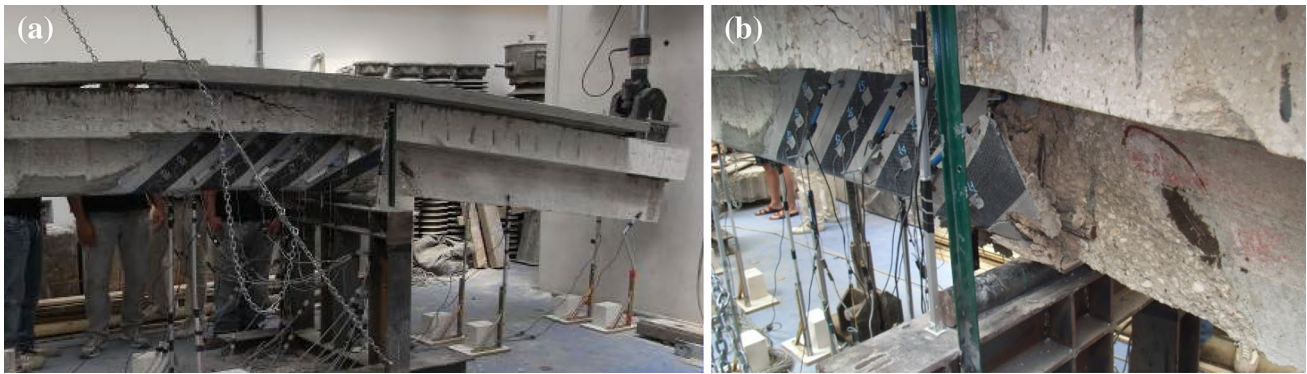
Fig. 15 Retrofitted beam S-TM1-A damage after the failure test; **a** damage at support B with negative moment; **b** detail of lateral ejection of concrete due to the interruption of the lower steel reinforcement
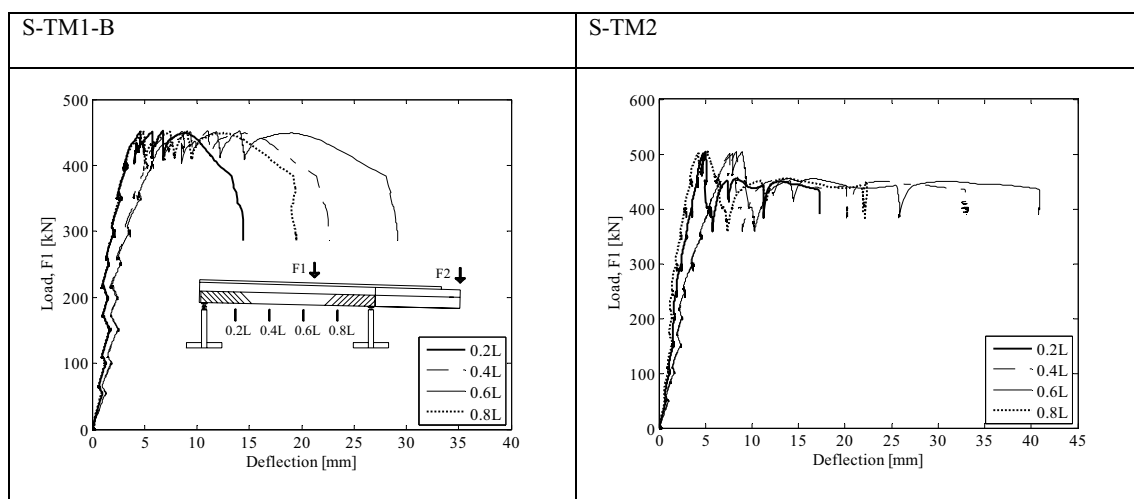
Fig. 16 Retrofitted beams S-TM1-B and S-TM2 experimental results of the failure test: load $F1$ vs span deflection curves at 0.2, 0.4, 0.6 and 0.8 L

therefore, the intervention proved to be effective. In fact, strips had a maximum strain of 1‰, sufficient to develop the additional shear contribution required.

The plain anchorage of the strips guaranteed the design shear strength even if it was applied, at least partially, on the cracked concrete zone.

This is an important conclusion as C-FRP plain anchorages are simpler to realize in situ, but international and national guidelines and code about C-FRP reinforcement, in case of complex load scheme (different from simple supported beam) do not give detailed information about how to calculate and realize C-FRP anchorages on cracked concrete.

In beam S-TM1-B, the greatest deformation had been measured at the middle level of the strip. Differently, the S-TM2 top and middle strip deformation were similar at the beginning, but then the middle deformations were smaller that the top ones. Top and middle deformations were again very similar at the end of the test. In both beams, the goal internal shear force was overtaken.

The final failure of shear reinforcement happened for debonding, probably due to strong compression deformations in concrete, together with tension in the strip. The simple evaluation of local strain in the strip does not allow to draw comprehensive conclusions concerning effectiveness. However, if we assume that a crack passes through strips 2 and 3, we may evaluate the contribution of the strips 2 and 3 with the measured maximum deformation $\varepsilon = 0.001$, each strip of two layers, the vertical C-FRP strip contribution in S-TM1-B is $V = 115$ kN. This is enough to guarantee the needed shear resistance.
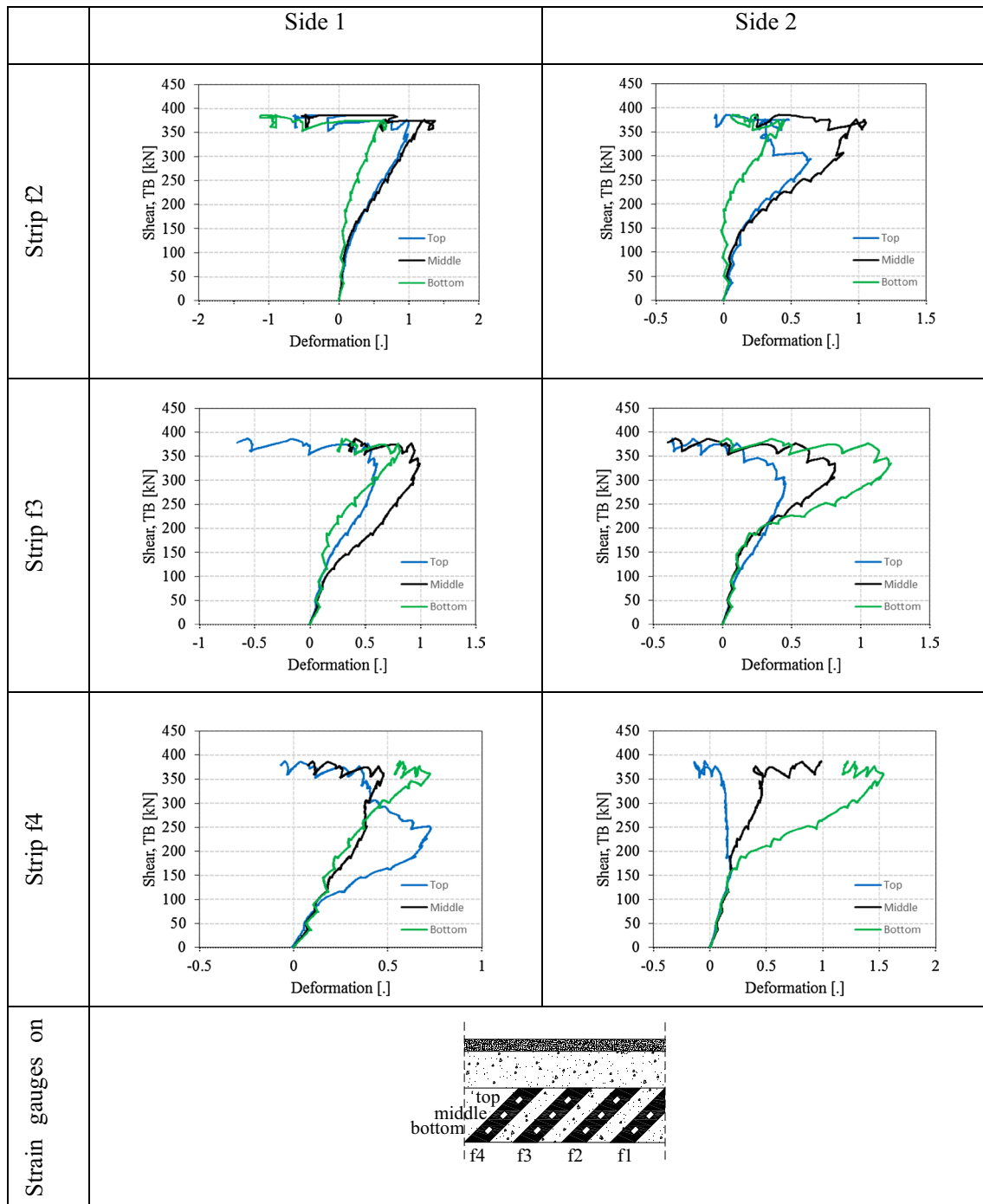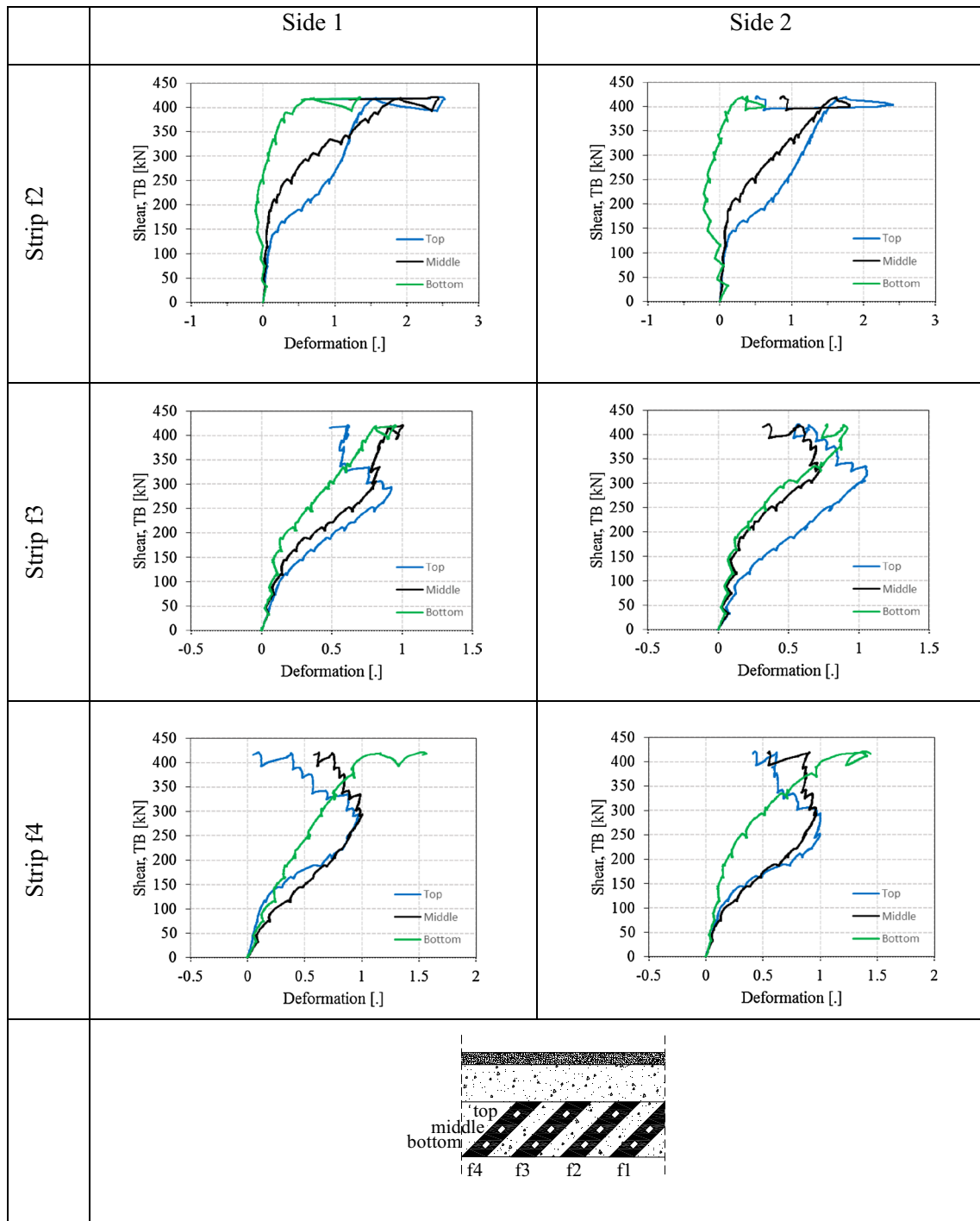
Fig. 17 Retrofitted beam S-TM1-B without retrofitting construction defects: shear at support B vs deformation curves for the C-FRP strips *f2*, *f3*, *f4* by strain gauges at the top, middle and bottom positions on each beam

Failure mechanism

The shear strengths of the two beam specimens S-TM1-B and S-TM2 were greater than the design one; therefore, it was proved that the retrofitting of the beam with C-FRP shear reinforcement was the exact solution. In fact, the collapse of beam occurred when the shear T_B and bending moment M_B at the support B were 384.86 kN and 396.00 kN m ($F1 = 450$ kN and $F2 = 165$ kN) or 416.49 kN and 396.00 kN m ($F1 = 500$ kN, $F2 = 165$ kN) for the beam S-TM1-B and S-TM2, respectively.

Fig. 18 Retrofitted beam S-TM2 without retrofitting construction defects: experimental results of the failure test; shear at support (TB) B vs deformation curves for the C-FRP strips *f2*, *f3*, *f4* by strain gauges at the top, middle and bottom positions on beam sides 1 and 2

The obtained shear values were greater than the design one of 206 kN and about two times the experimental shear strength of the specimen S-TM1-A (181 kN) with retrofitting defects. The beam part between simple supports without cantilever, where the *F*1 force was applied did not presented significant damage. The failure of the retrofitted beams was characterized (Figs. 19, 20) by:

- debonding of C-FRP strips (Figs. 19a, 20a);
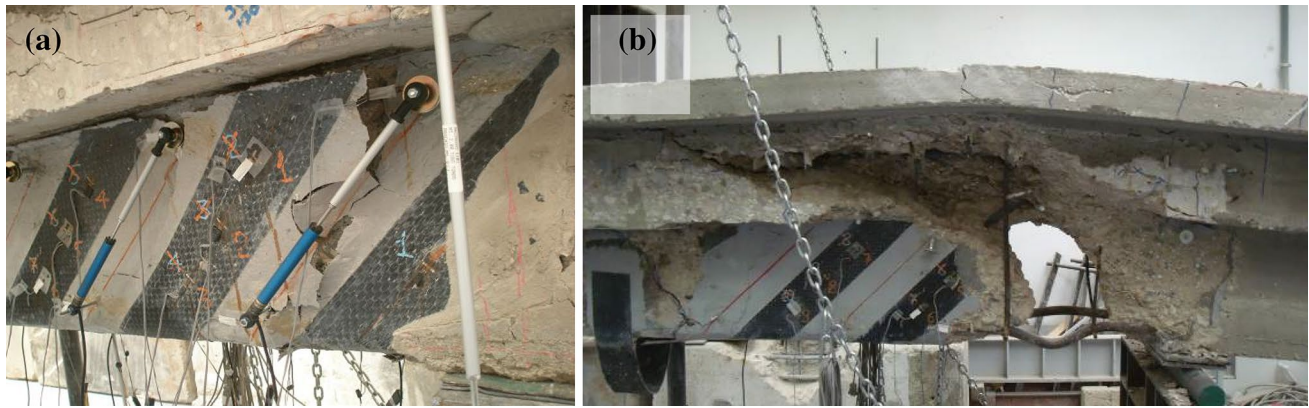
Fig. 19 Retrofitted beam S-TM1-B without retrofitting construction defects damage after the failure test: **a** debonding of C-FRP strips; **b** concrete diagonal crack and buckling of the longitudinal rebars near the support with negative moments
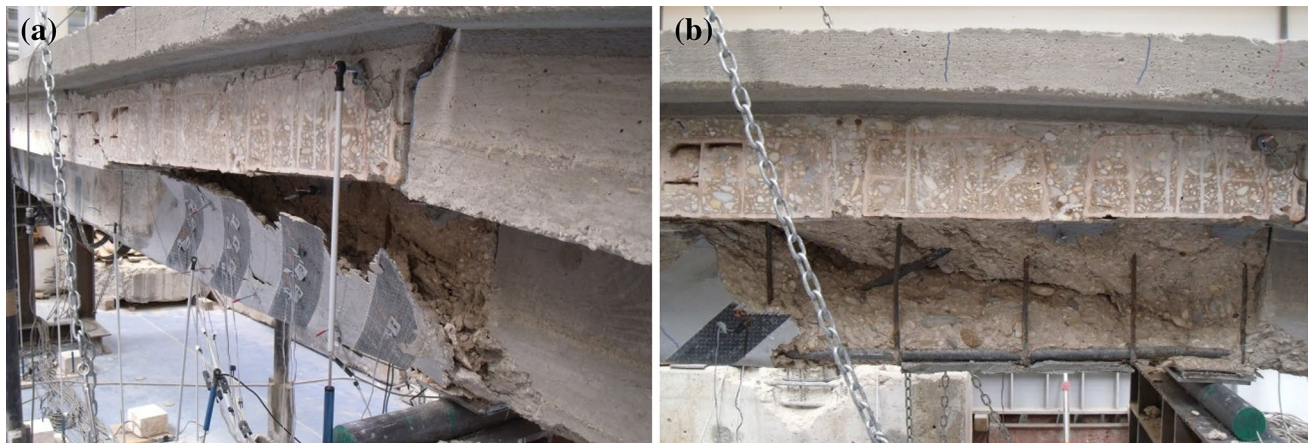
Fig. 20 Retrofitted beam S-TM2 without retrofitting construction defects: damage after the failure test **a** debonding of C-FRP strips; **b** concrete principal diagonal crack

- diagonal concrete cracks, passing through the two beam sides, which extend from the application point of the load $F1$ to the support B (Figs. 19b, 20b);
- buckling of the original rebars between the stirrups (Fig. 19b), for S-TM1-B only.

The damage sequence for the beams consisted in:

- one diagonal concrete crack from the original beam slab, in the section, where $F1$ was applied, to the C-FRP strip $f4$ and debonding phenomena on $f4$ strip when the shear T_B was equal to about 251 kN and 210 kN for S-TM1-B and S-TM2, respectively ($F1 = 300$ kN and $F2 = 100$ kN for S-TM1-B, $F1 = 250$ kN and $F2 = 85$ kN for S-TM2). Some vertical cracks were evident on the slab near the support B in case of S-TM2;
- new diagonal concrete cracks on the two sides of the original beam slab and web and large C-FRP local deformations

when the shear in section B was equal to about 305 kN for each beam;
- diagonal cracks widening and evident debonding of the C-FRP strip at the top section near the support B when the shear was equal to about 373 kN.

Conclusions

Two beams (TM1 and TM2) extracted from an existing RC building located in Rome and dated around 1930 have been retrofitted in bending by adding an RC slab and reinforced in shear with C-FRP strips, using the same provisions adopted in the real building. The retrofitted beams have been tested until failure to investigate the shear strength of C-FRP-reinforced concrete when submitted to a stress state typical of a beam of a frame structure, in the presence of negative bending and shear. After the realization of the cantilever, to create negative bending and shear at one end

of the span, the retrofitting intervention consisted of two subsequent solutions. The beam TM1 had been first retrofitted as S-TM1-A specimen, but retrofitting provisions revealed unsatisfactory, due to premature fragile bending failure. A second retrofitting detailing was than applied to beam TM2, named S-TM2 beam specimen, and to a new intervention on TM1 on the opposite site, named S-TM1-B specimen. This second retrofitting detailing proved to be effective and was adopted.

The main conclusion of this study from the experimental evidence is that the shear strengthening of RC beams by externally bonded C-FRP sheets can be effective in providing additional shear resistance to existing members also for the analyzed loading scheme. The negative bending at the end of the cantilever, with the adopted provisions, does not render ineffective the shear reinforcement by U strips of C-FRP. When shear and negative bending develop simultaneously, shear cracks start from the beam extrados, supporting the FRP debonding if it is not adequately anchored. However, the simple C-FRP anchorages used for the retrofitted beams are resulted sufficient to guarantee the necessary shear strength improvement. In the first test on the beam S-TM1-A, debonding happened but for the crushing of compressed concrete at support B and not for cracking of the concrete in the tension zone of the section, where the C-FRP anchorages are applied. This failure could be easily avoided with a proper design of the compressed reinforcement. Each section of the retrofitted beam should show a ductile behavior until failure after the retrofitting intervention as crushing of compressed concrete and rebar buckling can produce debonding of the C-FRP shear reinforcement. This should be a serious concern in concrete frame retrofitting, and becomes even of larger consequences if C-FRP U strips are adopted.

S-TM1-A had some further inadequate detailing which reduced both the overall and the local ductility, related to flexural behavior or anchoring of connection between the new slab and the old beam. In the case at hand, the presence of not well-engineered solutions reduced the foreseen shear resistance to at least 50%.

The second interventions tested in lab with the realization of the specimen S-TM1-B and S-TM2, with the simple modification of some construction and retrofitting detailing, avoided brittle flexural failure and the detachment of the new slab assuring the target shear and bending strength. These beams showed more than doubled experimental shear resistances with respect to the one of the S-TM1-A beam. It was showed that, even in the presence of negative bending, the use of U C-FRP strips, without any particular anchorage provision, can solve possible needs of retrofitting. It seems obvious that the only real proof is a test like the one here presented.

Finally, this paper provides original experimental results, because the tested beams, removed from an existing building, give an effective evaluation of the strengthening intervention as in real-framed structures, where the shear forces are combined with negative moments at supports. The obtained experimental results significantly improve the database of full-size beams, available from literature, with flexural strengthening and shear FRP reinforcements.

References

Adhikary B, Mutsuyoshi H (2004) Behavior of concrete beams strengthened in shear with carbon-fiber sheets. J Compos Constr 8(3):258–264

Albanesi T, Lavorato D, Nuti C, Santini S (2008) Experimental tests on repaired and retrofitted bridge piers. In: Proceedings of the international FIB symposium 2008—tailor made concrete structures: new solutions for our society, p 151

Albanesi T, Lavorato D, Nuti C, Santini S (2009) Experimental program for pseudodynamic tests on repaired and retrofitted bridge piers. Eur J Environ Civ Eng 13(6):671–683. https://doi.org/10.1080/19648189.2009.9693145

Barros JAO, Dias SJE (2006) Near surface mounted CFRP laminates for shear strengthening of concrete beams. Cem Concr Compos 28:276–292

Bousselham A, Chaallal O (2008) Mechanism of shear resistance of concrete beams strengthened in shear with externally bonded FRP. J Compos Constr 12(5):499–512

Carolin A, Taljsten B (2005) Experimental study of strengthening for increased shear bearing capacity. J Compos Constr 9(6):488–496

CNR-DT 200 R1/2013 (2013) Istruzioni per la Progettazione, l'Esecuzione ed il Controllo di Interventi di Consolidamento Statico mediante l'utilizzo di Compositi Fibro-rinforzati. Materiali, strutture di c.a. e di c.a.p., strutture murarie" **(in Italian)**

FIB (2001) Design and use of externally bonded FRP reinforced polymer reinforcement (FRP EBR) for reinforced concrete structures. FIB bulletin 14, Lausanne, Switzerland

Fiore A, Spagnoletti G, Greco R (2016) On the prediction of shear brittle collapse mechanisms due to the infill-frame interaction in RC buildings under pushover analysis. Eng Struct 121:147–159. https://doi.org/10.1016/j.engstruct.2016.04.044 **(ISSN:0141-0296)**

Fiorentino G, Forte A, Pagano E, Sabetta F, Baggio C, Lavorato D, Nuti C, Santini S (2017) Damage patterns in the town of Amatrice after

August 24th 2016 Central Italy earthquakes. Bull Earthq Eng. https://doi.org/10.1007/s10518-017-0254-z

Forte A, Santini S, Fiorentino G, Lavorato D, Bergami AV, Nuti C (2018) Influence of materials knowledge level on the assessment of the shear strength characteristic value of existing RC beams. In: 12th fib international Ph.D. symposium in civil engineering, August 29–31, 2018, Prague, Czech Republic

Garcez M, Meneghetti L, da Silva Pinto, Filho LC (2008) Structural performance of RC beams poststrengthened with carbon, aramid and glass FRP systems. J Compos Constr 12(5):522–530

Guadagnini M, Pilakutas K, Waldron P (2006) Shear resistance of FRP RC beams: experimental study. J Compos Constr 10(6):464–473

Imperatore S, Lavorato D, Nuti C, Santini S, Sguerri L (2012a) Shear performance of existing reinforced concrete T-beams strengthened with FRP. In: Proceedings of the 6th international conference on FRP composites in civil engineering, CICE 2012

Imperatore S, Lavorato D, Nuti C, Santini S, Sguerri L (2012b) Numerical modeling of existing RC beams strengthened in shear with FRP U-sheets. In: Proceedings of the 6th international conference on FRP composites in civil engineering, CICE 2012

Imperatore S, Lavorato D, Nuti C, Santini S, Sguerri L (2013a) Shear behavior of existing RC T-beams strengthened with CFRP. Assessment, upgrading and refurbishment of infrastructures, IABSE symposium report, 6 May 2013, vol 99, no 18, pp 958–965(8)

Imperatore S, Lavorato D, Nuti C, Santini S, Sguerri L (2013b) Shear behavior of existing RC T-beams strengthened with CFRP. Assessment, upgrading and refurbishment of infrastructures, Padova, ITA

Italian Council of Public Works (2009) Guidelines for design, execution and testing of reinforcement interventions for reinforced and/or prestressed concrete structures and walls using FRP (**In Italian**)

Khalifa A, Nanni A (2000) Improving shear capacity of existing RC T-section beams using CFRP composites. Cem Concr Compos 22(3):165–174

Lavorato D, Nuti C (2010) Seismic response of repaired bridges by pseudodynamic tests. In: Bridge maintenance, safety, management and life-cycle optimization—Proceedings of the 5th international conference on bridge maintenance, safety and management, pp 2368–2375

Lavorato D, Nuti C (2011) Pseudo-dynamic testing of repaired and retrofitted RC bridges. In: fib symposium PRAGUE 2011: concrete engineering for excellence and efficiency, Proceedings, 1, pp 451–454

Lavorato D, Nuti C (2015) Pseudo-dynamic tests on reinforced concrete bridges repaired and retrofitted after seismic damage. Eng Struct 94:96–112. https://doi.org/10.1016/j.engstruct.2015.01.012

Lavorato D, Nuti C, Santini S (2010) Experimental investigation of the seismic response of repaired RC bridges by means of pseudo-dynamic tests. In: Large structures and infrastructures for environmentally constrained and urbanised areas, pp 448–449. https://www.scopus.com/inward/record.uri?eid=2-s2.0-84929000824%26partnerID=40%26md5=add6f8195da5644cf25a15da84bee3bb

Lavorato D, Nuti C, Santini S, Briseghella B, Xue J (2015) A repair and retrofitting intervention to improve plastic dissipation and shear strength of Chinese RC bridges. In: Proceedings of IABSE conference—structural engineering: providing solutions to global challenges September 23–25 2015, Geneva, Switzerland

Lavorato D, Bergami AV, Forte A, Quaranta G, Nuti C, Monti C, Santini S (2016) Influence of materials knowledge level on the

assessment of the characteristic value of the shear strength of existing RC beams. In: Proceedings of Italian concrete days 2016, October 27–28, 2016, Rome, Italy

Lavorato D, Bergami AV, Nuti C, Briseghella B, Xue J, Tarantino A, Marano G, Santini S (2017a) Ultra-high-performance fibre-reinforced concrete jacket for the repair and the seismic retrofitting of italian and chinese RC bridges. In: COMPDYN 2017 6th ECCOMAS thematic conference on computational methods in structural dynamics and earthquake engineering. Rhodes Island, Greece, 15–17 June 2017

Lavorato D, Vanzi I, Nuti C, Monti G (2017b) Generation of non-synchronous earthquake signals. In: Gardoni P (eds) Risk and reliability analysis: theory and applications. Springer, Cham, pp 169–198. https://doi.org/10.1007/978-3-319-52425-2_8

Marano GC, Pelliciari M, Cuoghi T, Briseghella B, Lavorato D, Tarantino AM (2017) Degrading Bouc–Wen model parameters identification under cyclic load. Int J Geotech Earthq Eng 8(2):60–81. https://doi.org/10.4018/IJGEE.2017070104

Monti G, Liotta MA (2007) Tests and design equations for FRP-strengthening in shear. Constr Build Mater 21:799–809

NTC (2008) "Norme Tecniche per le Costruzioni", DM 14.01.2008, Ministero dei Lavori Pubblici, Gazzetta Ufficiale della Repubblica Italiana, 29

Nuti C, Santini S, Sguerri L (2010) Experimental tests on FRP shear retrofitted RC beams. In: CICE 2010—conference on composites in civil engineering, Beijing, China

Nuti C, Santini S, Sguerri L (2014) In situ shear-tearing test for the quality control on FRP-to-concrete bonded joints. In: Proceedings of the 7th international conference on FRP composites in civil engineering, CICE 2014

OPCM (Ordinanza del Presidente del Consiglio dei Ministri) (2003) OPCM 3274 (20/03/2003): first elements concerning general criteria for the seismic classification of the national territory and technical norms for structures in seismic zone (Primi elementi in materia di criteri generali per la classificazione sismica del territorio nazionale e di normative tecniche per le costruzioni in zona sismica) (in Italian). OPCM, Rome

Pellegrino C, Modena C (2000) Fiber-reinforced polymer shear strengthening of reinforced concrete beams with transverse steel reinforcement. J Compos Constr 6(2):104–111

Trifunac MD, Todorowska MI (1997) Response Spectra for differential motion of columns. Earthq Eng Struct Dyn 26(2):251–268

Zhang Z, Hsu CTT (2005) Shear strengthening of reinforced concrete beams using carbon-fiber-reinforced polymer laminates. J Compos Constr 9(2):158–169

Zhou Z, Nuti C, Lavorato D (2014) Modeling of the mechanical behavior of stainless reinforcing steel. In: Proceedings of the 10th fib international Ph.D. symposium in civil engineering, pp 515–520

Zhou Z, Lavorato D, Nuti C, Marano GC (2015) A model for carbon and stainless-steel reinforcing bars including inelastic buckling for evaluation of capacity of existing structures. In: COMPDYN 2015—5th ECCOMAS thematic conference on computational methods in structural dynamics and earthquake engineering, pp 876–886